ASME Journal of Biomechanical Engineering
Online journal at:
https://asmedigitalcollection.asme.org/biomechanical

Development of a Portable Low-Cost System for the Metrological Verification of Wheelchair Roller Ergometers

Matteo Lancini
Medical and Surgical Specialties,
Radiological Sciences and Public Health Department,
University of Brescia,
Via Branze 38, Brescia 25123, Italy

Paolo Spada
Medical and Surgical Specialties,
Radiological Sciences and Public Health Department,
University of Brescia,
Via Branze 38, Brescia 25123, Italy

Ridi Muhametaj
Medical and Surgical Specialties,
Radiological Sciences and Public Health Department,
University of Brescia,
Via Branze 38, Brescia 25123, Italy
e-mail: matteo.lancini@unibs.it

Rick de Klerk
Center for Human Movement Sciences,
University Medical Center Groningen,
University of Groningen,
Antonius Deusinglaan 1,
Groningen 9713 AV, The Netherlands

Lucas H. V. van der Woude
Center for Human Movement Sciences,
University Medical Center Groningen,
University of Groningen,
Antonius Deusinglaan 1,
Groningen 9713 AV, The Netherlands

Riemer J. K. Vegter
Center for Human Movement Sciences,
University Medical Center Groningen,
University of Groningen,
Antonius Deusinglaan 1,
Groningen 9713 AV, The Netherlands
e-mail: r.j.k.vegter@umcg.nl

Wheelchair ergometers are widely used in research, clinical practice, and sports environments. The majority of wheelchair ergometers are roller systems that allow for wheelchair propulsion in the personal wheelchair on one or two (instrumented) rollers. Oftentimes these systems are only statically calibrated. However, wheelchair propulsion is dynamic by nature, requiring a dynamic validation process. The aim of the current project was to present a low-cost portable system for the dynamic metrological verification of wheelchair roller ergometers, based on an instrumented reference wheel. The tangential force on the roller is determined, along with its uncertainty, from the reference wheel properties, and compared with the force measured by the ergometer. Uncertainty of this reference wheel system was found to be lower than the one of the ergometer used, indicating that this novel approach can be used for the metrological verification of ergometers.
[DOI: 10.1115/1.4062810]

Manuscript received January 30, 2020; final manuscript received June 5, 2023; published online July 12, 2023. Assoc. Editor: Sudeep Sastry.

1 Introduction

1.1 State of the Art. The ergometric assessment of handrim wheelchair propulsion is essential for research [1,2], clinical practice, and sports environments [3–5] as it can be used to optimize the wheelchair, wheelchair user, and the wheelchair-user interface [6]. As a result, wheelchair ergometry and wheelchair ergometers are an active topic of research [2,6].

A wide variety of ergometers has been developed over the past decades; however, in recent years, there is a renewed interest in roller ergometers as they provide a number of advantages over other designs [2]. The main advantage of these ergometers is that they provide the opportunity to measure the wheelchair user in their personal wheelchair while simultaneously collecting data on their power output and propulsion technique. Moreover, in contrast to treadmills, they also allow for sprint testing [7] and require no additional equipment for measuring kinetics. The main outcome measures for a wheelchair ergometer are the torque and velocity. For the purpose of this paper, the measured torque applied by the wheelchair-user on the roller of the ergometer is viewed as the primary outcome measure of the system.

Calibration and validation of ergometers is always required regardless of the origin or type of the ergometer [8]. The force component at the interface between wheel and ground, which is particularly relevant for most studies involved in propulsion, could be considered an alternative expression of the torque measured. Using this quantity, most of the variables (e.g., peak/mean force, push/cycle time, etc.) relevant to handrim wheelchair propulsion research can be computed [9,10]. Force transducers are usually calibrated and validated in static condition, since a high accuracy at low-cost is achievable using gravity and known masses, usually with a static force or torque applied. The working conditions of ergometers, however, are far from static: rolling resistance and inertial parameters change with speed and affect the measurement; therefore a mechanical verification should involve testing in dynamic conditions, with torque and forces changing over time and a non-null speed closer to the actual working conditions.

Devices for cycling applications were subject to numerous studies, focusing more on repeatability than traceability; an unbroken chain of comparisons to stated references. The calibration of bicycle ergometers has been shown to contain errors for different types of ergometers [11,12]. They are usually validated with a reference mobile power meter for cycling, comparing only power output measured by both under steady-state conditions. However, these tests cannot be directly applied to wheelchair ergometers as calibrators or reference devices are not widely available.

The current paper proposes a low-cost metrological reference system to verify the correct measurement of the contact force at the

wheel-roller interface of a roller ergometer. The uncertainty of the proposed approach is determined using a set of international norms [13]. This has been used to demonstrate the capability of the system to test an existing wheelchair ergometer.

1.2 Proposed Approach. The current paper proposes a cantilever system containing a wheel with a variable inertial mass as a dynamic verification system. The system should be low-cost to allow any lab to reproduce the setup without having a manufacturer involved. It must also be portable to allow for interlaboratory comparison of different ergometers. Currently calibration is performed by the manufacturer and adjusted using proprietary setups in static conditions, but a proper metrological chain of reference to allow comparison is rare, due to the difficulties of having a traveling reference standard suitable for this particular application, which is dynamical in nature.

The proposed approach focuses on a reference device, able to apply a known tangential force on the ergometer roller at different rotational speeds. The idea is based on three different applications of a coast-down test, with a wheel of known inertial properties. On every test, the wheel is to be driven up to a known speed, then decoupled from its motor source, and slowed down without external contribution. This will allow the assessment of the forces inducing a deceleration from the profile of the rotational speed of the wheel over time.

The first test is used to characterize the reference wheel itself. During the first test, the wheel is free-standing, only to be slowed down by air and internal friction associated with the system. In the second test, the wheel will be in contact with the roller of the ergometer, but no resisting torque is applied by the ergometer. In this way, the contributions of the rolling resistance as a function of speed and vertical load can be assessed. Finally, in the third test, the wheel will be counteracted by the ergometer, which can be juxtaposed to the behavior of the wheel in the first two tests.

2 Methods

2.1 Instrumented Wheel. The designed system is a device which produces forces at the ergometer roller edge using its own inertia during deceleration. The guidelines followed during the design of the system were:

(i) cost: to limit the overall cost of the system
(ii) availability: to use off-the-shelf components
(iii) portability: to ensure the system could travel between different labs

This structure (Fig. 1) consists of a 24 in. (0.61 m) rear bike wheel (model Alexrims ace 19) positioned on vertical slider guides attached to a support aluminum structure. These guides allow the addition of weights to push the wheel downwards with a known force. The wheel was connected to a brushless servomotor (BMH0703T11F2A, Schneider Electric, France) with a declared speed of 2000 rpm and maximal torque of 3.1 Nm. However, it should be noted that almost any motor would suffice. The motor controls the speed of the bike wheel and drives it through a freewheel system which allows for a mechanical decoupling of the motor torque from the wheel by inverting the rotation of the motor.

At the rim, cylindrical brass masses (Fig. 1) can be clamped at regular intervals to allow varying the inertia of the wheel. The masses were primarily designed to allow for easy installation on the system. In fact, it is possible to attach and detach them without removing the wheel from the cantilever system using hex keys.

The system was equipped with a position sensor based on a low-cost custom-made phonic wheel. A standard bike brake disk coupled with a photocell was used for this purpose (model MOCH25A, Kingbright, Taiwan). The acquisition system (NI9411 by NI, Austin, TX) acquires the phonic wheel signal at 25 kHz, and provides a trigger signal to the ergometer's datalogger. The phonic wheel was calibrated against an encoder using a lookup table, as

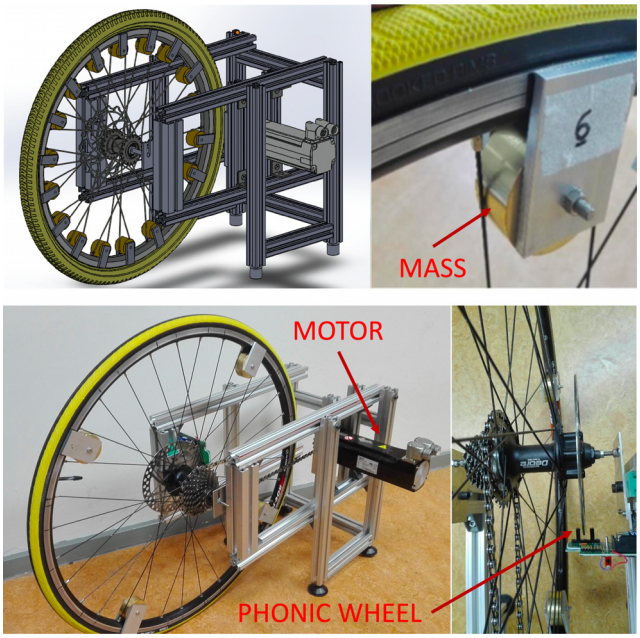

Fig. 1 Instrumented cantilever wheel for ergometer metrological validation (reference wheel). The mechanical design (upper left side), a detail of the additional masses (upper right side), a full picture of the device (bottom left side), and a detail of the position sensor(phonic wheel, bottom right side).

suggested in Ref. [14], resulting in a 0.1 rad uncertainty on the angular position.

The cost of the position and speed sensor is about 30€, and the bike wheel is a commercial spare part costing less than 40€, while the support structure was internally realized for a total of about 100€of materials and handiwork. The motor chosen was already available, but a cheaper version could be procured for about 200€. NI hardware (National Instruments Corporation, Austin, TX) was used as it was already available in the laboratory, but any data acquisition hardware, already available in the lab, could be used. The overall weight of the system depends on the number of additional masses connected, but is between 6 kg (2 kg wheel + 3 kg motor + 1 kg structure) and about 17 kg(+ 4 kg for the vertical load mass and + 0.4 kg for each brass mass added, up to 16).

2.2 Mathematical Model. The external motor was used to drive the wheel up to the desired velocity, then it was disconnected using a common biking freewheel system. This results in a coast-down with no forces acting on the wheel other than those dependent on the mechanical properties of the wheel (friction, inertia, etc.) and those associated with the tangential force applied by the ergometer.

The proposed method relies on the solution of the dynamical equilibrium of the wheel to describe the wheel angular acceleration $\dot{\omega}$ as a polynomial function of the rotational velocity ω, as shown in the following equation:

$$\dot{\omega}(t) = -k\omega(t)^2 - c\omega(t) - \alpha \tag{1}$$

where k is a parameter related to the squared rotational velocity, c to the linear rotational velocity, and α is independent from the velocity. These variables assume different meanings in the three different test configurations (see below) and are used to assess the desired quantities. The value of k, c, and α for each test are obtained with a numerical solver (a Gauss–Newton algorithm, which implements a nonlinear least square regression, developed in MATLAB), minimizing the error between the measured angle and the estimated one.

2.2.1 Configuration 1: Stand-Alone Tests. The mechanical model is depicted in Fig. 2, with the wheel modeled as a rigid disk

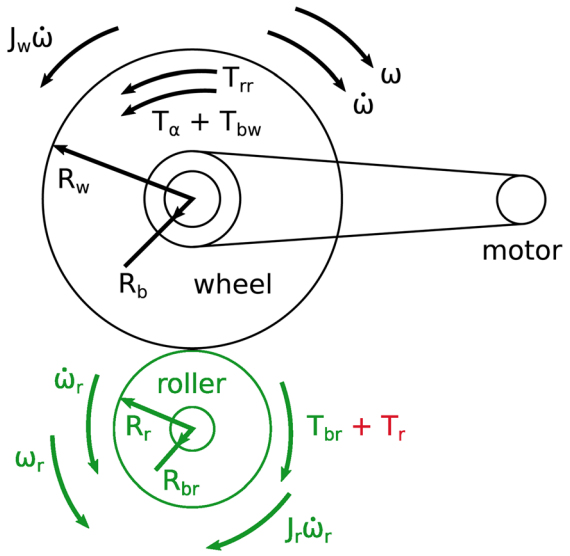

Fig. 2 Mechanical model of the wheel with the components of the standalone configuration in black, the additional elements of the zero-torque configuration in light gray, and the additional element for the vairable torque configuration denoted T_r in light gray. T_a, resistance torque due to the air friction; T_{bw}, resistance torque of the wheel bearings; $\dot{\omega}$, wheel angular acceleration; ω, wheel angular velocity; J_w, wheel moment of inertia; ωr, roller angular velocity; $\dot{\omega}_r$, roller angular acceleration; T_{rr}: rolling resistant torque, T_{br}, resistant torque due to roller bearing's friction; T_r, motor's resistant torque.

of radius R_w in a bi-dimensional space. Three forces are considered acting on the wheel: T_a, the torque associated with air friction, T_{bw}, the torque due to the rolling friction of the wheel bearings, and $J_w\dot{\omega}$, due to the moment of inertia J_w of the wheel.

Since no other forces are acting, the equilibrium of the torques is given by the following equation:

$$J_w\dot{\omega} = -T_a - T_{\text{bw}} \tag{2}$$

Here, $T_{bw} = f_b R_b g M_w$ is the bearings friction torque, and $T_a = C_w\omega^2$ is the torque associated with the drag. If we define M_w as the wheel mass (including the masses added to increase inertia), R_b the bearing radius, C_w an aerodynamic factor (combining drag factor, air density and area), f_b the bearing friction coefficient, respectively, we can rewrite Eq. (2) as the following equation

$$\dot{\omega} = -\frac{C_w}{J_w}\omega^2 - \frac{f_b R_b g M_w}{J_w} \tag{3}$$

This allows us to define the parameters k_{SA} and α_{SA} for 1, which will be the results of the first set of tests, as specified in Eq. (4), where the "SA" subscript identifies parameters assessed during stand-alone tests. c_{SA} is null since there is no linear contribution (see Eq. (4))

$$k_{\text{SA}} = \frac{C_w}{J_w} \quad c_{\text{SA}} = 0 \quad \alpha_{\text{SA}} = \frac{f_b R_b g M_w}{J_w} \tag{4}$$

2.3 Configuration 2: Zero-Torque Mode. The second set of tests was used to assess the dissipative actions that are due to internal elements and rolling resistances [15] caused by the interaction between the ergometer and the wheel. The roller of the ergometer in this configuration is set as completely passive, with no active torque except the resisting torque offered by the friction of the roller bearings and its inertia.

The mechanical model associated with this configuration is shown in Fig. 2, with respect to the standalone model, we have the addition of T_{br}, the torque due to the roller bearings, J_r, the inertia of the roller, and T_{rr}, the rolling resistance of the wheel associated with the deformation of the tire.

The dynamic equilibrium at the wheel can be expressed by transferring the T_{br} and J_r terms from the roller to the wheel, as shown in the following equation:

$$J_w\dot{\omega} = -T_a - T_{\text{bw}} - J_r\dot{\omega}\left(\frac{R_w}{R_r}\right)^2 - T_{\text{rr}} - T_{\text{br}}\frac{R_w}{R_r} \tag{5}$$

T_{rr} considers the rolling resistance as a dissipative-only phenomenon related linearly to the speed. While this is usually not the case in car and cycle applications, this assumption is valid at low speeds [16]. T_{rr} could be rewritten as a factor f_{rr} to be multiplied by ω. A separate friction factor f_{br} is instead assumed on the roller bearings. Concerning the forces transmitted, the wheel bearing are working in a different way: the wheel mass M_w is fully supported by the roller and the wheel bearings are pushed down by an external additional load M_v. The force acting on the wheel bearing is now just $M_v g$, the vertical force between wheel and roller is $(M_v + M_w)g$, and the force acting on the roller bearing is given by $(M_v + M_w + M_r)g$, where M_r is the mass of the roller.

Following the same approach as earlier, the dynamic equation could be rewritten as a differential equation governing angular acceleration, as shown in the following equation:

$$\begin{aligned}\dot{\omega} = &-\frac{C_w}{J_w + J_r\left(\frac{R_w}{R_r}\right)^2}\omega^2 - \frac{f_{rr}}{J_w + J_r\left(\frac{R_w}{R_r}\right)^2}\omega \\ &- \frac{T_{\text{bw}} + f_{\text{br}}R_{\text{br}}(M_w + M_v + M_r)g\frac{R_w}{R_r}}{J_w + J_r\left(\frac{R_w}{R_r}\right)^2}\end{aligned} \tag{6}$$

With the parameters of Eq. (1) assuming the values shown in Eq. (7), where the "ZT" suffix indicated that they are assessed using the zero-torque tests

$$\begin{aligned}k_{\text{ZT}} &= \frac{C_w}{J_w + J_r\left(\frac{R_w}{R_r}\right)^2} \quad c_{\text{ZT}} = \frac{f_{rr}}{J_w + J_r\left(\frac{R_w}{R_r}\right)^2} \\ \alpha_{\text{ZT}} &= \frac{T_{\text{bw}} + f_{\text{br}}R_{\text{br}}(M_w + M_v + M_r)g\frac{R_w}{R_r}}{J_w + J_r\left(\frac{R_w}{R_r}\right)^2}\end{aligned} \tag{7}$$

2.3.1 Configuration 3: Full Model (Variable Torque). The last configuration used was the closest to the actual working condition of the ergometer: the wheel is applied on the roller, which provides a resistive torque thanks to its motor or brake.

This configuration, shown in Fig. 2, is similar to the zero-torque mode, with the only addition of a constant resistive torque T_r actively generated by the ergometer, which can be set at different constant values thanks to the ergometer controller. The dynamic equilibrium, similarly to the previous case, could be described by the following equation:

$$J_w\dot{\omega} = -T_a - T_{\text{bw}} - J_r\dot{\omega}\left(\frac{R_w}{R_r}\right)^2 - (T_{\text{br}} + T_r)\frac{R_w}{R_r} - T_{\text{rr}} \tag{8}$$

Applying the same substitutions as before, the differential equation describing angular acceleration can be rewritten as shown in the following equation:

$$\dot{\omega} = -\frac{C_w}{J_w + J_r\left(\frac{R_w}{R_r}\right)^2}\omega^2 - \frac{f_{rr}}{J_w + J_r\left(\frac{R_w}{R_r}\right)^2}\omega + \\ -\frac{T_{bw} + f_{br}R_{br}(M_w + M_v + M_r)g\frac{R_w}{R_r} + T_r\frac{R_w}{R_r}}{J_w + J_r\left(\frac{R_w}{R_r}\right)^2} \tag{9}$$

With the parameters of Eq. (1) assuming the values shown in Eq. (10), where the "VT" suffix indicated that they are applicable to the variable-torque tests

$$k_{VT} = \frac{C_w}{J_w + J_r\left(\frac{R_w}{R_r}\right)^2} \quad c_{VT} = \frac{f_{rr}}{J_w + J_r\left(\frac{R_w}{R_r}\right)^2} \\ \alpha_{VT} = \frac{T_{bw} + f_{br}R_{br}(M_w + M_v + M_r)g\frac{R_w}{R_r} + T_r\frac{R_w}{R_r}}{J_w + J_r\left(\frac{R_w}{R_r}\right)^2} \tag{10}$$

It can be noticed that, given the same vertical load condition, and the same inertia, $k_{VT} = k_{ZT}$, as well as $c_{VT} = c_{ZT}$.

2.4 Tangential Force Assessment. The tangential force F_t that is exchanged between wheel and roller can be obtained by considering that F_t, multiplied by the wheel radius, must equal the torques acting on the wheel, as shown in the following equation:

$$F_t R_w = J_w\dot{\omega} + T_{bw} + T_a + T_{rr}\omega \tag{11}$$

$$F_t = \frac{J_w\dot{\omega} + f_b R_b g M_v + C_w\omega^2 + f_{rr}\omega}{R_w} \tag{12}$$

Therefore, it is possible to compute the value of the tangential force, as shown in Eq. (12), starting from the rolling resistance (computed from the c value the zero-torque mode), the air friction and the wheel bearings friction (computed from k_{SA} and α_{SA}), the wheel radius R_w and its inertia J_w.

First, the values of α, k, and c are obtained by fitting experimental data in all three different configurations. Then, the wheel bearings friction f_b is estimated using the value of α_{SA}, the rolling resistance coefficient f_{rr} is estimanted using c_{ZT}; finally, the active resistance torque of the roller T_r is estimated from $c_{V\,T}$.

2.5 Testing

2.5.1 Measurement Uncertainty. In order to provide a reliable validation, the uncertainty associated with the reference measurement should be less than the uncertainty of the measurement system of interest. To guarantee this condition, an uncertainty budget was computed for every test configuration following the standard approach suggested by the Joint Committee for Guides in Metrology [13].

2.5.2 Protocol. Trained observers (PS, RM) performed all tests in the three described configurations (Standalone, Zero Torque, Variable Torque), with different working parameters. The parameters taken into account were:

(1) the inertia of the wheel, set by adding 0, 4, 8, or 16 masses of about 0.3 kg each to the wheel
(2) the initial speed of the wheel, set to 10, 15, or 20 km/h
(3) the vertical mass on the wheel axis, set using only the wheel weight or adding an additional 4 kg to its axle
(4) the active resistance of the roller, set to 0.1, 0.2, 0.3, or 0.5 Nm

The coast-down tests were repeated five times for each combination of parameters. During tests in standalone configuration there was no contact between the wheel and the roller, so only the inertia and the initial speed of the wheel were taken into account, totaling 16 combinations repeated five times each. During tests in zero-torque mode the resistance torque of the roller is null, therefore only the other three parameters were changed, for a total of 24 combination repeated five times each. In the full test with variable torque all the four parameters were taken into account, with a total of 96 combinations repeated five times each.

For each variable-torque test, the quantities depending on previous tests, were estimated by averaging the α, k, c values resulting from the curve fitting of the zero-torque and standalone tests having the same parameters combination.

2.5.3 Estimation of Inertia. The moment of inertia of the wheel, in its four different configurations (0, 4, 8, and 16 masses), was measured using the trifilar pendulum method [17] and a motion capture system (Optotrak, NDI, Canada). All the masses (the inertial masses of the wheel, the wheel mass, the vertical mass) were weighted using a laboratory weighing scale. The dimensions of the wheel and of the roller were measured directly, while the friction coefficients and the dimensions of the bearing were extracted from their data sheets and their relative uncertainty was assumed to be about 1%.

2.5.4 Ergometer Testing. The ergometer used to demonstrate the method capability was an Esseda computer-controlled servo-driven dual-roller ergometer [18] developed by Lode BV (Groningen, The Netherlands) in close collaboration with the University Medical Center Groningen (UMCG, Groningen, The Netherlands). Everyday and sports wheelchairs can be mounted on the ergometer and secured with four tie-downs. User generated bi-manual forces are transferred through the roller-motor assembly to a load-cell. The model tested was a development prototype, lacking certain filter options and other improvements hereafter introduced to improve accuracy.

The ergometer has a number of different modes to measure wheelchair specific performance. In the current paper, the zero-torque and iso-inertial mode were used. In the zero-torque (freewheel) mode, the ergometer is fully passive with only internal friction and inertia acting on the roller. In the iso-inertial mode, the ergometer simulates overground propulsion according to a simple mechanical model of wheelchair propulsion in an admittance-control feedback loop. This is the most commonly used mode. As such, this mode was used for testing in the variable torque condition.

To highlight any difference due to the dynamic calibration, the ergometer was statically calibrated before the tests.

The ergometer datalogger acquires data at 70 Hz. The error is computed as the difference between the instantaneous values of the tangential force $F_{t,ergo}$ measured by the ergometer and the same value $F_{t,wheel}$ assessed by the instrumented wheel (downsampled to make comparisons easier). The deceleration phase is identified using the phonic wheel described earlier in the paper (to detect the end of the phase when the wheel speed is lower than 0.1 rad/s, based on the resolution of the phonic wheel) and the signal from the motor controller (the phase starts 1 s after the disconnection of the motor).

3 Results

3.1 Measurement Uncertainty. Table 1 shows all known and measured parameters' values, along their standard uncertainties. The uncertainty of the measurement of the wheel angular velocity depends on the number of divisions and the calibration performed as in Ref. [14], resulting in a value of 0.02 rad/s at 20 km/h. The uncertainty associated with the parameters α, k, c obtained by fitting experimental data was assessed using the residuals of the fit, following the approach previously suggested in Ref. [19]. For all three parameters, the relative standard uncertainty ranged from 3%

Table 1 Values and uncertainties of the evaluated parameters

Parameter	Unit	Value	Uncertainty	
Roller b. r.	mm	16.64	0.02	0.1%
Wheel b. r.	mm	47.1	0.5	0.1%
Wheel r.	mm	299.5	0.3	0.1%
Roller r.	mm	50.1	0.3	0.6%
Vertical masses	g	3905	2	0.04%
Brass masses	g	399.0	0.5	0.1%
Roller mass	kg	13.96	0.14	0.1%
Wheel mass	kg	2.04	0.02	1%
Roller b. fr.		0.05	0.0005	1%
moment of i. 1	$kg\,m^2$	0.11		0.1%
moment of i. 2	$kg\,m^2$	0.22		0.9%
moment of i. 3	$kg\,m^2$	0.34		0.3%
moment of i. 4	$kg\,m^2$	0.56		0.2%

b, bearings; fr., friction; *r*., radius; *i*., inertia.

to 23%, depending on the configuration and the parameters combination.

The uncertainty associated with the tangential force was assessed as combined uncertainty of all parameters present in Eq. (12), following the standard approach suggested in Ref. [13]. The combined uncertainty of the tangential force, $U_{95\%}(F_{t,\text{wheel}})$, was extended to a 95% level of confidence. In all tests, this extended uncertainty ranged between 0.05 and 0.15 N, depending on the actual speed and the test condition.

The value of the residual errors measured (see Table 2) is consistently higher than the value of the uncertainty of the measurement wheel, meaning that the error is not due to the uncertainty of the measurement wheel, but statistically significant.

A typical result of this comparison is shown in Fig. 3, which shows the tangential force measured by the ergometer and by the cantilever system along with its confidence interval. To provide an indicator of the overall quality of the encoder measurement, the root-mean-square of the error was determined for each test condition, taking

Table 2 Root mean square error (*N*) of the tangential force measured by the ergometer, with respect to the force assessed by the cantilever wheel assumed as reference

Resistant torque (Nm)			0.1	0.2	0.3	0.5
IM	VL (N)	TS (km/h)	RMS error (*N*)			
0	0	20	1.3	1.2	1.8	1.5
0	0	15	1.5	1.3	1.4	1.7
0	0	10	1.6	1.5	*	*
0	39	20	1.2	1.1	1.1	1.2
0	39	15	1.7	1.3	1.4	1.2
0	39	10	1.7	*	*	*
4	0	20	1.2	1.0	1.0	1.1
4	0	15	1.4	0.9	1.0	1.2
4	0	10	1.6	1.3	1.4	*
4	39	20	1.8	1.3	0.9	1.2
4	39	15	1.2	1.0	0.9	*
4	39	10	1.4	1.5	*	*
8	0	20	1.6	0.8	0.8	1.8
8	0	15	1.3	0.8	0.8	1.3
8	0	10	1.3	1.5	*	*
8	39	20	1.6	0.9	0.9	1.8
8	39	15	1.3	0.7	0.8	1.0
8	39	10	1.2	*	1.2	*
16	0	20	1.5	2.0	0.8	1.4
16	0	15	1.4	1.1	0.9	2.4
16	0	10	1.4	0.9	1.3	*
16	39	20	1.4	0.9	0.8	1.8
16	39	15	1.2	0.9	0.9	1
16	39	10	1.2	0.8	0.8	*

IM, additional inertial masses; VL, vertical load; TS, top speed; *, the test was too short to perform an assessment (the wheel stopped too early).

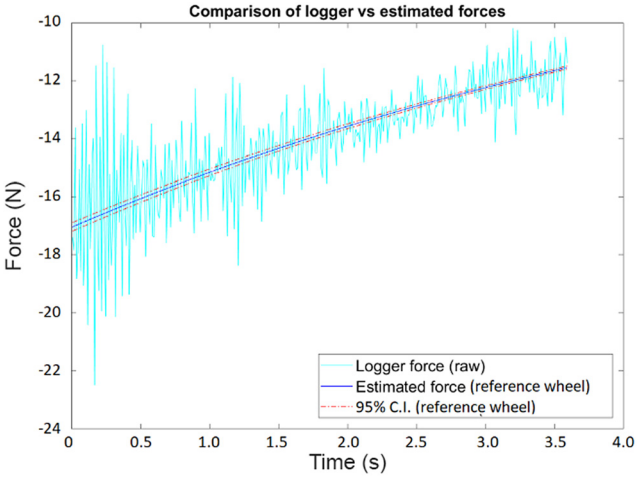

Fig. 3 Example of a comparison between ergometer and reference wheel data at an initial velocity of 20 km/h, no masses added and a resistant torque of 0.1 Nm

into account data recorded from the when the wheel starts to decelerate to its complete stop. Table 2 reports the average results for all the tests performed. It should be noted that, since the ergometer was already statically calibrated, this is a further error associated with the dynamic condition, and that each result reported in Table 2 is the RMS combination of 5 repetitions.

To provide an even more synthetic evaluation of the quality of the measurement of the tangential force by the ergometer, an ordinary linear regression between all the $F_{t,\text{wheel}}$ values in every tests and the same $F_{t,\text{ergo}}$ values was computed, resulting in a regression standard error $\sigma_0 = 1.9N$, which amounts to about 9% of the maximum force tested, and less than 1% of the ergometer full scale.

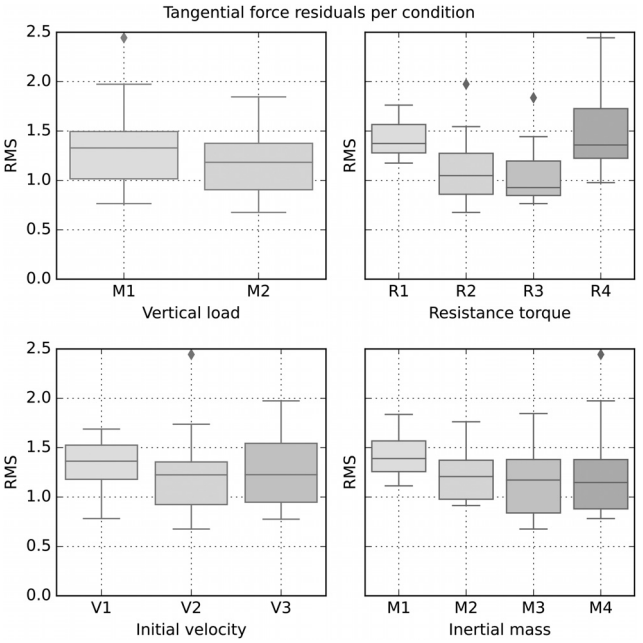

Fig. 4 Sensitivity of the tangential force residuals with respect to the variables investigated: vertical load, resistant torque, initial velocity, and inertial mass. The boxplots report the median, the II and III quartile and the whiskers extend to 1.5 of the interquartile distance. Outliers were identified as outside this range. The average of each dataset is indicated as a dotted line. Outliers are indicated by the * symbol. No significant difference between the groups were identified using a paired *t*-test.

Tests with a high resistant torque and a low top speed display the highest values, probably due to the short time needed for the wheel to completely stop, resulting in less data points available for evaluation, and a less stable behavior. For the same reason, some tests were not considered valid, since the data available for fitting was not enough to provide an estimate.

3.2 Sensitivity With Respect to Investigated Variables. Since different conditions lead to similar results in term of errors, the sensitivity of the error with respect to different parameters used to define the tests was investigated. Figure 4 shows the variation of the residuals of the tangential force with respect to the different testing conditions. As can be noticed that all conditions are compatible and depict a similar performance of the ergometer, and this has been confirmed by a paired *t*-test between group pairs.

4 Discussion

The constructed device achieved its aim of being low-cost, using available components, and being portable while proving its use to determine the validity of a wheelchair roller ergometer. The estimated cost of the system is estimated to be lower than 400€. To the best knowledge of the authors, a power meter for wheelchairs could cost about 5 times that amount, with a compatible accuracy. Both systems would require specific expertise to analyze the data and implement the proposed approach. The validation, however, would be occasional, and could involve a trained technician, as is common in calibration of measurement instruments in many fields.

A general practice in metrological calibration of measurement systems is that the reference should be associated with a measurement uncertainty lower than the one of the device being tested. This allows to neglect the uncertainty contribution of the validation system in the comparison between the two systems. In our case, the combined uncertainty of the validation system was approximately ten times lower than the uncertainty of the ergometer used as a demonstration. Satisfying this requirement could be difficult with a more accurate ergometer: a lower uncertainty of the reference wheel parameters, especially its inertia, would also be required to validate such system.

An example in the case of the ergometer used in this work could be that if the manufacturer introduces a filter to reduce the noise and improve results in the commercial version, then the validation system should be improved as well. Applying a low-pass filter to the ergometer signal would be recommended in this case as the frequency content of wheelchair propulsion kinetics is less than 10 Hz [20].

The system presented in this paper can be used to calibrate and compare systems with a relative uncertainty sensibly higher than 1%, which is generally associated with consumer devices and not with clinical devices. The proposed method, however, could be adapted improving its accuracy to adapt the reference to more accurate devices.

The main contributors to the combined uncertainty of the tangential force are the speed measurement, which has an uncertainty percentage contribution of 90% in slower conditions, and the inertia measurement, which reached a similar level at higher speeds. The reference wheel could be improved by using a different encoder. The custom-made encoder was low-cost, while a new disk or a industrial encoder could avoid irregularities in the speed data. The inertia of the wheel as determined by the trifilar pendulum had a relatively large uncertainty compared to its value (about 1% to 5%). The determination of inertia could be improved by accelerometric measurements, employing torque meters or by replacing the wheel with a homogeneous disk.

Another limitation is the applied vertical load during the tests, which is lower than a wheelchair-user combination on the ergometer. However, the loading of the system did not appear to influence the uncertainty of the system, and increasing the vertical load would require a heavier and less portable system. Systems that allow for heavier loading can be based on this system if cost and portability are de-emed less important. An ergometer with no iso-inertial mode could also raise some issues since it would be impossibile to decouple the roller resistance from the motor resistance, but this could be addressed by looking at the specific mode of functioning of such ergometer.

The reference wheel can be used for metrological verification of roller ergometers. This could also be done between labs as the system is portable and low-cost to ensure compatibility between results obtained from different ergometers/institutes, which is especially relevant for the field of wheelchair propulsion, where sample sizes are generally low. It can be used to assess the long-term stability of an ergometer by performing multiple measurements over the span of multiple weeks or months. The method described could be used to further improve and adapt the system for devices with higher accuracy, higher loads or different speeds.

Acknowledgment

The authors would like to thank Davide Battini, and Gabriele Coffetti for the lab support in Brescia and Emyl Smid and Wim Kaan for the lab support in Groningen.

Funding Data

- Samenwerkingsverband Noord-Nederland, Ministerie van Economische Zaken (Award No. OPSNN0109; Funder ID: 10.13039/501100003195).
- PPP-allowance of the Top consortia for Knowledge and Innovation of the Ministry of Economic Affairs.

Data Availability Statement

The datasets generated and supporting the findings of this article are obtainable from the corresponding author upon reasonable request.

References

[1] Mason, B. S., Vegter, R. J. K., Paulson, T. A. W., Morrissey, D., van der Scheer, J. W., and Goosey-Tolfrey, V. L., 2018, "Bilateral Scapular Kinematics, Asymmetries and Shoulder Pain in Wheelchair Athletes," Gait Posture, **65**, pp. 151–156.

[2] De Klerk, R., Vegter, R., Goosey-Tolfrey, V., Mason, B., Lenton, J., Veeger, H., and Van Der Woude, L., 2020, "Measuring Handrim Wheelchair Propulsion in the Lab: A Critical Analysis of Stationary Ergometers," IEEE Rev. Biomed. Eng., **13**, pp. 199–211.

[3] van der Scheer, J. W., de Groot, S., Vegter, R. J., Veeger, D. H., and van der Woude, L. H., 2014, "Can a 15m-Overground Wheelchair Sprint Be Used to Assess Wheelchair-Specific Anaerobic Work Capacity?," Med. Eng. Phys., **36**(4), pp. 432–438.

[4] Goosey-Tolfrey, V. L., Vegter, R. J. K., Mason, B. S., Paulson, T. A. W., Lenton, J. P., van der Scheer, J. W., and van der Woude, L. H. V., 2018, "Sprint Performance and Propulsion Asymmetries on an Ergometer in Trained High- and Low-Point Wheelchair Rugby Players," Scand. J. Med. Sci. Sports, **28**(5), pp. 1586–1593. may

[5] de Groot, S., Bos, F., Koopman, J., Hoekstra, A. E., and Vegter, R. J. K., 2018, "The Effect of a Novel Square-Profile Hand Rim on Propulsion Technique of Wheelchair Tennis Players," Appl. Ergon., **71**, pp. 38–44.

[6] van der Woude, L. H., Veeger, H. E., Dallmeijer, A. J., Janssen, T. W., and Rozendaal, L. A., 2001, "Biomechanics and Physiology in Active Manual Wheelchair Propulsion," Med. Eng. Phys., **23**(10), pp. 713–733.

[7] Hutzler, Y., 1998, "Anaerobic Fitness Testing of Wheelchair Users," Sports Med., **25**(2), pp. 101–113.

[8] DiGiovine, C. P., Cooper, R. A., and Boninger, M. L., 2001, "Dynamic Calibration of a Wheelchair Dynamometer," J. Rehabil. Res. Dev., **38**(1), pp. 41–55.

[9] Veeger, H. E., and van der Woude, L. H., and Rozendal, R. H., 1989, "Wheelchair Propulsion Technique at Different Speeds," Scand. J. Rehabil. Med., **21**(4), pp. 197–203.

[10] Vegter, R. J., Lamoth, C. J., de Groot, S., Veeger, D. H., and van der Woude, L. H., 2014, "Inter-Individual Differences in the Initial 80 Minutes of Motor Learning of Handrim Wheelchair Propulsion," PLoS One, **9**(2), p. e89729.

[11] Abbiss, C. R., Levin, G., McGuigan, M. R., and Laursen, P. B., 2008, "Reliability of Power Output During Dynamic Cycling," Int. J. Sports Med., **29**(7), pp. 574–578.

[12] Maxwell, B. F., Withers, R. T., Ilsley, A. H., Wakim, M. J., Woods, G. F., and Day, L., 1998, "Dynamic Calibration of Mechanically, Air- and Electromagnetically Braked Cycle Ergometers," Eur. J. Appl. Physiol. Occup. Physiol., **78**(4), pp. 346–352.

[13] JCGM, 2008, "Evaluation of Measurement Data–Guide to the Expression of Uncertainty in Measurement," JCGM, **100**(2008), pp. 1–116.
[14] Tan, K. K., Zhou, H. X., and Lee, T. H., 2002, "New Interpolation Method for Quadrature Encoder Signals," IEEE Trans. Instrum. Meas., **51**(5), pp. 1073–1079.
[15] Theisen, D., Francaux, M., Fay, A., and Sturbois, X., 1996, "A New Procedure to Determine External Power Output During Handrim Wheelchair Propulsion on a Roller Ergometer: A Reliability Study," Int. J. Sports Med., **17**(8), pp. 564–571.
[16] Curtiss, W., 1969, "Low Power Loss Tires," SAE Paper No. 690108.
[17] Hughes, G., 1957, "Trifilar Pendulum and Its Application to Experimental Determination of Moments of Inertia," ASME Paper No. 57-SA-51.
[18] De Klerk, R., Vegter, R., Veeger, H., and Van der Woude, L., 2020, "Technical Note: A Novel Servo-Driven Dual-Roller Handrim Wheelchair Ergometer," IEEE Trans. Neural Syst. Rehabil. Eng., **28**(4), pp. 953–960.
[19] Kennedy, M. C., and O'Hagan, A., 2001, "Bayesian Calibration of Computer Models," J. R. Stat. Soc. Ser. B: Stat. Methodol., **63**(3), pp. 425–464.
[20] DiGiovine, C. P., Cooper, R. A., DiGiovine, M. M., Boninger, M. L., and Robertson, R. N., 2000, "Frequency Analysis of Kinematics of Racing Wheelchair Propulsion," IEEE Trans. Rehabil. Eng., **8**(3), pp. 385–393.